SLEEPJ, 2018, 1–10

doi: 10.1093/sleep/zsy176
Advance Access publication Date: 1 September 2018
Original Article

ORIGINAL ARTICLE

Lateralized rhythmic acoustic stimulation during daytime NREM sleep enhances slow waves

Péter Simor[1,*], Emilie Steinbach[2], Tamás Nagy[1], Médhi Gilson[2], Juliane Farthouat[2], Rémy Schmitz[2], Ferenc Gombos[3,4], Péter P. Ujma[5,6], Miklós Pamula, Róbert Bódizs[5,6] and Philippe Peigneux[2]

[1]Institute of Psychology, Eötvös Loránd University, Budapest, Hungary, [2]UR2NF—Neuropsychology and Functional Neuroimaging Research Group at CRCN—Center for Research in Cognition and Neurosciences and UNI—ULB Neurosciences Institute, Université Libre de Bruxelles (ULB), Brussels, Belgium, [3]Department of General Psychology, Pázmány Péter Catholic University, Budapest, Hungary, [4]MTA-PPKE Adolescent Development Research Group, Budapest, Hungary, [5]Institute of Behavioural Sciences, Semmelweis University, Budapest, Hungary and [6]National Institute of Clinical Neurosciences, Budapest, Hungary

The work was performed at UR2NF—Neuropsychology and Functional Neuroimaging Research Group at CRCN—Center for Research in Cognition and Neurosciences and UNI—ULB Neurosciences Institute, Université Libre de Bruxelles (ULB), Brussels, Belgium.

*Corresponding author. Peter Simor, Institute of Psychology, Eötvös Loránd University, Budapest, Hungary. Email: simor.peter@ppk.elte.hu.

Abstract

Slow wave sleep (SWS) is characterized by the predominance of delta waves and slow oscillations, reflecting the synchronized activity of large cortical neuronal populations. Amongst other functions, SWS plays a crucial role in the restorative capacity of sleep. Rhythmic acoustic stimulation (RAS) during SWS has been shown a cost-effective method to enhance slow wave activity. Slow wave activity can be expressed in a region-specific manner as a function of previous waking activity. However, it is unclear whether slow waves can be enhanced in a region-specific manner using RAS. We investigated the effects of unilaterally presented rhythmic acoustic sound patterns on sleep electroencephalographic (EEG) oscillations. Thirty-five participants received during SWS 12-second long rhythmic bursts of pink noise (at a rate of 1 Hz) that alternated with non-stimulated, silent periods, unilaterally delivered into one of the ears of the participants. As expected, RAS enhanced delta power, especially in its low-frequency components between 0.75 and 2.25 Hz. However, increased slow oscillatory activity was apparent in both hemispheres regardless of the side of the stimulation. The most robust increases in slow oscillatory activity appeared during the first 3–4 seconds of the stimulation period. Furthermore, a short-lasting increase in theta and sigma power was evidenced immediately after the first pulse of the stimulation sequences. Our findings indicate that lateralized RAS has a strong potential to globally enhance slow waves during daytime naps. The lack of localized effects suggests that slow waves are triggered by the ascending reticular system and not directly by specific auditory pathways.

Statement of Significance

Delta waves and slow oscillations (SOs) appear to play a critical role in the restorative functions of sleep. Recent findings suggest that rhythmic acoustic stimulation (RAS) can entrain and synchronize cortical oscillations and hence, increase slow oscillatory activity during deep sleep. Here we examined the influence of unilaterally presented repetitive sound bursts on cortical oscillations during daytime sleep. We found a robust and global increase in slow oscillatory activity regardless of the side of the stimulation. Nevertheless, delta waves and SOs show a certain degree of refractoriness after sustained stimulation. RAS is noninvasive, easily applicable and cost-effective procedure. Our findings provide new insights into the potential and limitations of this promising technique.

Key Words: neural entrainment; delta power; slow oscillations; slow wave sleep; auditory stimulation; laterality

Submitted: 1 April, 2018; **Revised:** 4 July, 2018

Introduction

Slow wave sleep (SWS) is characterized by the predominance of low frequency electroencephalographic (EEG) oscillations (called delta waves, range 0.5–4 Hz) reflecting the synchronized activity of large cortical neuronal populations [1]. These oscillations emerge from the activity of thalamo-cortical and cortico-cortical networks, in which widely distributed neurons synchronously and rhythmically alternate between hyperpolarized "down states" and depolarized "up states" [2, 3]. In the range of delta activity, slow oscillations (SOs, large, >75 mV amplitude waves around 1 Hz frequency) are the most prominent feature of SWS sleep. SOs seem to originate from neocortical regions, and are known to play a key role in the restorative functions of sleep [4–6]. The extent and integrity of SOs are predictive of improved cognitive functions, such as enhanced learning and memory consolidation [7].

A growing number of studies showed that SOs can be artificially boosted using several techniques including pharmacological and transcranial direct current or magnetic stimulation (see Bellesi *et al.* [8] for an extensive review). Although these approaches provide means to manipulate and examine the effects of SOs in experimental settings, their utility and applicability in clinical and field studies remain limited. In this context, rhythmic acoustic stimulation (RAS) during sleep is a promising new procedure that is cost-effective, easily applicable, noninvasive, and highly efficient in increasing SOs and delta power [8]. Two main RAS approaches have been applied so far: closed-loop, phase-locked stimulation [9, 10] and neural entrainment [11, 12]. Whereas closed-loop stimulation consists of providing sound stimuli during the up-states of the SOs, neural entrainment aims at synchronizing neural activity to a predefined acoustic rhythm (~1 Hz), that is, presenting the auditory stimulation sequence irrespective of the phase of the ongoing oscillations. Recent studies suggest that beyond augmenting SOs and delta power, RAS contributes to sleep-dependent, declarative memory consolidation both in healthy individuals [9, 13] and participants at risk for sleep- and memory-related impairments [14, 15].

Another interesting feature of delta power and SOs is their localized, region-specific expression: although slow oscillatory activity is detectable in the whole cortex, relative increases of slow wave activity (SWA) preferentially appear at cortical locations that were previously "exposed" to higher information-processing demands [16, 17]. At a more global level, hemispheric asymmetries in slow oscillatory activity were also reported specifically during SWS, suggesting that one cerebral hemisphere may remain more alert, and responsive to environmental inputs during the deepest stage of sleep [18, 19].

In light of these findings, our aim was to examine the effects of lateralized RAS during daytime sleep on hemispheric slow waves. A series of rhythmic (1 Hz) tone sequences was delivered through headphones into one of the ears of the participants as soon as they entered stabile stage 2 sleep. Repeated 12-second long stimulation sequences were followed by silent periods lasting 15 seconds. Based on prior results, delta power expected to increase during the stimulated periods in contrast to the silent ones. In addition, we hypothesized a local-dependent RAS effect; that is, higher increase in delta power localized in the targeted side. In other terms, we predicted a relatively greater enhancement of delta power in the hemisphere contralateral to the stimulated ear.

Methods

Participants

We recruited participants through public announcements at the Université Libre de Bruxelles (ULB, Belgium). We invited them to spend a daytime nap in the sleep laboratory of the ULB Neuropsychology and Functional Neuroimaging Research Group (UR2NF). Exclusion criteria included left-handedness [20] and prior or current psychiatric, neurological, chronic somatic disorders, as well as signs of depressive symptoms (Beck's Depression Scale ≥ 12, Beck *et al.* [21]), sleep complaints (Pittsburgh Sleep Quality Index ≥ 8, Buysse *et al.* [20]) as measured by standard questionnaires. Participants were asked to follow regular sleep schedules for at least 1 week before the experiment. Compliance was verified by daily sleep logs. In addition, they were instructed to go to bed 1 hour after and to wake up 1 hour before their usual sleep schedule, to increase the probability of falling asleep in the laboratory. Additionally, we asked them to refrain from drinking caffeinated, stimulant or alcoholic drinks the day before and the day of the study. Data of 19 participants were excluded as they did not sleep enough, or were aroused by external noise and could not receive the minimal amount of acoustic stimulation (i.e. six sequences, see below). The daytime sleep EEG data of 35 individuals (15 males, mean age = 27.25, *SD* = 5.3) who spent at least 10 minutes in stabile NREM sleep was analyzed. Participants received monetary compensation (30 EUR) for taking part in the experiment. The study procedure was carried out in accordance with the Declaration of Helsinki. The Ethical Committee of the Université Libre de Bruxelles approved the study protocol and participants gave written informed consent to the procedure.

Acoustic stimulation

Stimuli were generated using a custom-made software tool (FerciosSoundGenerator, Ferenc Gombos 2015). Sequences of acoustic stimulation consisted of 12 bursts of pink noise delivered for 12 seconds (1 Hz stimulation frequency). A continuous pink noise was amplitude-modulated by a sinusoidal function that generated oscillating sound patterns with rising and falling flanks, respectively (Figure 1). This way, the sound bursts lasting 1000 ms reached their maximal intensity at 500 ms. Sound stimulation was presented monaurally through in-ear headphones RHAS500u (RHA Technologies, Glasgow, Scotland). We measured the sound volume prior to each experiment using a sound level meter (Voltcraft SL451, Conrad Electronic SE, Hirschau, Germany). Volume was individually set to the lowest level that the participants could still detect during resting wakefulness. Stimulation sequences lasting 12 seconds alternated with 15 seconds of silent, baseline periods.

Procedure

Participants arrived in the laboratory at 12:00 pm. After verification of the sleep diaries, they were fitted with Ag/AgCl electrodes at eight scalp locations following the 10–20 international system (F3, F4, C3, C4, T3, T4, P3, and P4 referenced to the average of the mastoids M1 and M2) [23]. Electrooculography (EOG) and submental electromyogram (EMG) with bipolar references were also obtained in order to detect eye movements and muscle-related

artifacts, respectively. Impedances were kept below 5 kΩ. Signals were collected, amplified and digitized at 2048 Hz sampling rate with 24-bit resolution using the DC coupled Biosemi 256 channel AD-box (BioSemi B. V., Amsterdam). For EEG and EOG recordings, (off-line) high-pass and low-pass frequency digital filters were set at 0.10 and 48 Hz, respectively. EMG high-pass and low-pass frequency filters were set at 10 and 100 Hz, respectively.

Participants had the opportunity to spend a daytime nap between 01:00 pm and 03:00 pm in a quiet, dark room. A researcher trained in sleep staging continuously monitored the EEG recordings of the participants from an adjacent room. Acoustic stimulation was initiated whenever the participants spent at least 5 minutes in NREM sleep (stage 2 or SWS) uninterrupted by awakenings, arousals or stage shifts (except the transition from stage 2 to SWS). Sound sequences that alternated with silent periods were delivered using a custom-made script, written in Matlab (Mathworks, Natick, MA). The side of the stimulation was randomized across participants. Thus, each participant received the sounds only in one of his/her ears during the entire nap. The intensity of the sound was increased in a stepwise manner: starting from the individually adjusted lowest volume, we gradually increased the intensity of the simulation by 5% in each sequence, but stimulation did never exceed 60 dB. After reaching this limit, the intensity was quasi-randomly modulated between the lower and upper range. However, the volume of the sound bursts was always the same within a sequence. Our aim with this modulated volume protocol was to minimize habituation to repeated, identical stimuli [8]. The stimulation was paused if the researcher detected any sign of awakening, arousals, or if the participant was no longer in NREM sleep. Stimulation was resumed (at the lowest volume) only if the participant reentered and spent at least 2 minutes in uninterrupted NREM sleep. Due to inter-individual differences in sleep, the number of RAS and corresponding silent trials varied across participants (mean = 63.25, *SD* = 32.47, range = 6–130). Participants woke up spontaneously or were awoken by the experimenter, who debriefed them about the nature of the study, and removed the electrodes. None of the included participants reported to notice the sounds during the nap.

Data processing

To verify whether the stimulation was delivered during stage 2 and SWS, sleep recordings were scored off-line according to standardized criteria [24]. An expert in sleep research performed sleep staging using a custom-made software tool for sleep EEG analysis (FerciosEEGPlus, Ferenc Gombos 2008–2017). EEG data were processed with custom-written Matlab codes using the fieldtrip toolbox [25]. Sleep EEG recordings were preprocessed, band-pass filtered between 0.3 and 40 Hz (Butterworth, zero phase forward and reverse digital filter), and downsampled (to 256 Hz). Sequences of RAS, and corresponding silent periods of stage 2 and SWS were selected for further analysis. Silent segments were defined as the 12 seconds preceding the onset of RAS segments. As silent periods lasted 15 seconds, the 3 seconds bordering each RAS and corresponding silent periods were discarded from the analysis. The first silent period, that is, the 12

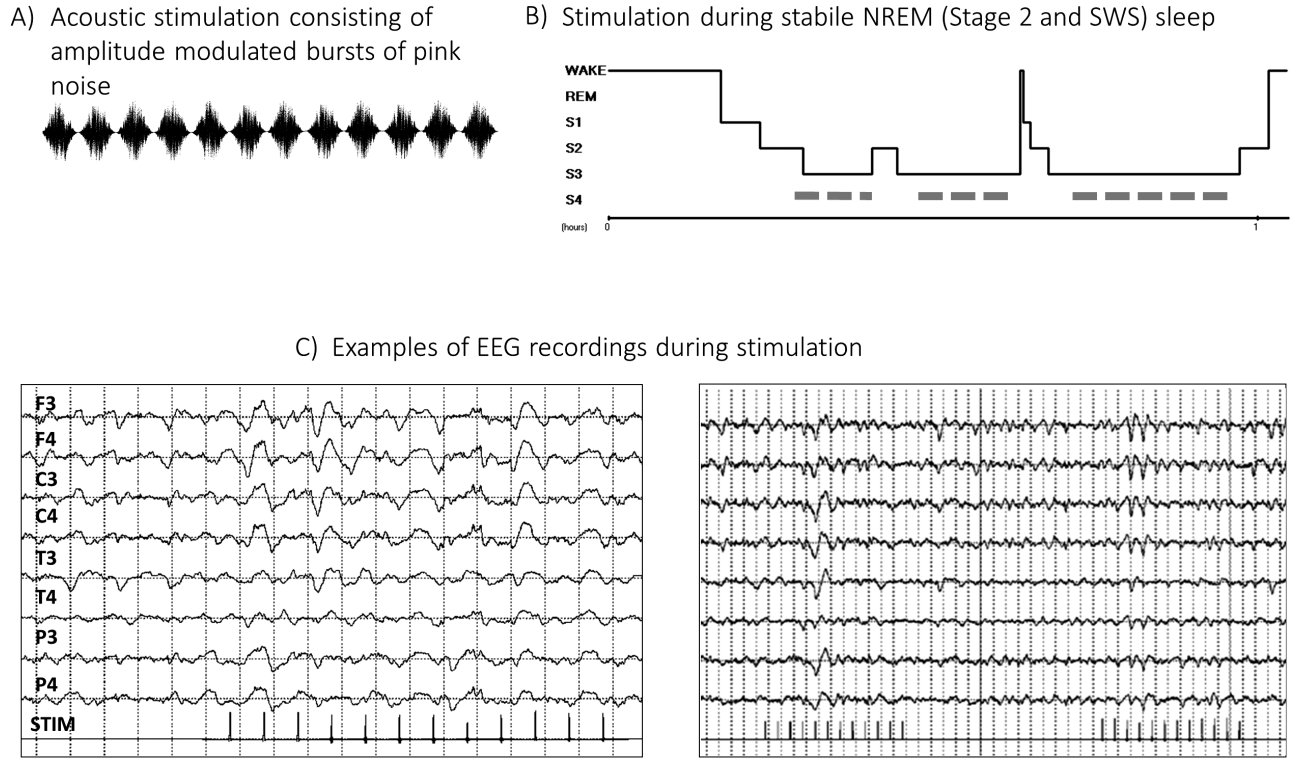

Figure 1. Stimulation procedure. (A) One RAS sequence lasted 12 seconds, that alternated with silent periods lasting 15 seconds. Amplitude-modulated pink noise was delivered in bursts of 1 Hz frequency. (B) Stimulation was initiated when participants entered into stabile, non-interrupted NREM sleep for a minimal duration of 5 minutes. Gray, dotted lines below the hypnogram indicate stimulation periods. (C) Examples of raw EEG data illustrating amplitude fluctuations during stimulation and silent segments within a shorter (left side) and a longer (right side) time window.

seconds preceding the first sequence of stimulation were not included in the analyses.

RAS and silent periods were transformed into 4-second long, overlapping (50%) segments. Technical and movement-related artifacts were visually inspected and removed before analysis. Hanning-tapered segments were Fourier Transformed with the FFT algorithm in order to obtain the average spectral power density (μV^2/0.25 Hz) of each stimulated and unstimulated trial (of 12-second duration) between 0.75 and 25 Hz with 0.25 Hz resolution. In addition, we computed the averaged spectral power values (including all trials) of RAS and silent periods, respectively. EEG data was log transformed and standardized (z-transformation) by participant prior to statistical analysis.

In order to analyze the temporal dynamics of rhythmic stimulation we carried out a time-frequency analysis contrasting stimulated and unstimulated trials. We performed frequency analysis (across the same frequency range, but with 1 Hz resolution) using a 1-second-long, Hanning-tapered time window sliding in steps of 50 ms over the 12-second long trials. The average time-frequency spectra for RAS and silent periods was obtained for statistical analysis.

To examine whether the ongoing EEG signal is synchronized to the rhythm of the repetitive acoustic stimulation, we performed two separate analyses.

First, we analyzed inter-trial phase coherence (ITPC) [26–28] within the RAS and silent trials. ITPC captures the consistency of phase angles (of each examined frequency) across trials in single electrodes. Furthermore, ITPC is independent of amplitude fluctuations. Values closer to 1 reflect high consistency (low variability) in phase angles across trials, whereas values around 0 indicate high variability of phase angles (no phase coupling) across the subsequent trials. As the presentation rate of acoustic bursts was stable across trials (12 bursts in 12 seconds with the same timing: 1 Hz), increased ITPC between RAS trials compared to silent segments would argue for the presence of phase coupling between the acoustic stimuli and the neural response. ITPC was computed for RAS and silent trials separately, based on the frequency analyses of 2-second Hanning-tapered time windows sliding in steps of 50 ms over the 12-second intervals.

Additionally, we performed an analysis of synchronization between the acoustic signal and the EEG channels. More specifically, we computed the coherence coefficient that quantifies phase synchrony between pairs of signals [29]. Coherence coefficients are the outputs of the cross-correlation function in the frequency domain. Normalized values range between 0 and 1. As the acoustic signal was delivered with a rate of 1 Hz, we computed only the coherence coefficients for this specific frequency. To measure the consistency of phase angles between the EEG channels and the auditory stimulation, the acoustic signal was preprocessed as follows: We downsampled the sampling rate of the acoustic signal to 256 Hz, and extracted the envelope of the sound bursts by computing the magnitude of the Hilbert transformed values. In addition, we applied a moving average filter to smooth the envelope of the signal (Supplementary Figure S2). To examine temporal changes in coherence coefficients we segmented the 12-second long trials to 50% overlapping, Hanning tapered, 4-second time windows, and used the FFT to extract the cross-spectral density of the channels of interest. This way we obtained the Coherence values for five time points (i.e. 12 seconds segmented by five 4 seconds overlapping windows). Values indicated the phase coherence between the envelope of the acoustic stimulation and the specific EEG channels within the examined frequency (1 Hz).

Statistical analysis

Statistical analyses were performed in R (R Core Team [30]). Our hypotheses assumed that (1) delta power (frequency spectra between 0.75 and 4 Hz) will increase during RAS in comparison with silent periods and (2) the increase during RAS will be relatively enhanced within the targeted hemisphere. In order to test these assumptions, we used linear mixed-effects modeling. The spectral power values of the specific bins were summed up to obtain the traditional frequency bands of delta (0.75–4 Hz), theta (4.25–8 Hz), alpha (8–12.75 Hz), sigma (13–15.75 Hz), and beta (16–25 Hz) frequency ranges, but bin-wise values were retained for exploratory analysis. In order to reduce the number of our variables, band-wise power values were averaged across electrode locations. Additionally, we averaged band-wise power values of the targeted and untargeted hemispheres, reflecting average spectral power values of electrode derivations contralateral and ipsilateral to the stimulated ear, respectively. This way, our main predictor variables were: condition (silence vs. RAS), side (untargeted vs. targeted), and band (delta, theta, alpha, sigma, and beta). Moreover, as the duration of stimulation showed considerable variability across participants—due to the dissimilar length of sleep—we included the variable Trial (number of sequences) as a confounding covariate. In order to select the random structure for the model we followed the recommendations of Zuur [31]. As a first step, we examined the fit of a linear regression model that consisted of the predictor variables condition, band, and side including all main effects and interactions. This model was used as a reference point, and was compared with a linear mixed-effects model that used random intercepts for the participant and the number of trials. Next, we created a random intercept (participant and trial number) and slope model, in which we assumed a random slope by the factor condition. Finally, we contrasted the model fits of the random intercept and the random intercept and slope models.

Post hoc comparisons of band-wise spectral power between RAS and silent conditions, and of the increase in spectral power (during RAS compared to silent periods) between Targeted and Untargeted sides were performed by paired *t*-tests or Wilcoxon-signed rank tests (if normality was violated) on power spectral values averaged across all trials. The issue of multiple comparisons was addressed by applying the Benjamin-Hochberg procedure to estimate false discovery rate.

As band-wise analysis might mask subtle differences in specific frequency bins that lie between the traditional frequency ranges, we performed (at an exploratory level) bin-wise comparisons contrasting spectral power between RAS and silent conditions, as well as spectral power increase between targeted and untargeted hemispheres. In order to reduce the number of statistical comparisons, spectral power values were averaged across channels and trials. As bin-wise data deviated from normality, statistical testing was performed by Wilcoxon-signed rank tests. This analysis included a large number of statistical comparisons (comparing 98 frequency bins). Therefore, we considered a difference statistically significant if at least three adjacent bins reached a threshold of $p < 0.05$ [32].

Time-frequency power and ITPC data were statistically analyzed by cluster-based nonparametric permutation test, that is, an

efficient method to deal with multiple comparisons in case of EEG data [33]. This procedure examines significant clusters of neighboring data points (in time and frequency), and compares the clusters of the observed data with those of a random distribution. Spectral power values at each time point and frequency bin (averaged across channels) were compared between RAS and silent conditions. Similarly, the same statistical plan (detailed below) was used to contrast the change in spectral power as a function of RAS within the targeted and untargeted hemispheres. Thus, we contrasted the average time-frequency power spectra of the targeted hemisphere during RAS divided by the average power spectra of targeted hemisphere during silent periods, with the average time-frequency power spectra of the untargeted hemisphere during RAS divided by the average power spectra of untargeted hemisphere during silent periods. Paired sample *t*-tests were computed for each pair of data (in each time point and frequency). Samples that exceeded a predefined alpha value ($p = 0.05$) were selected and clustered on the basis of spatial adjacency. The sum of the *t*-values within the clusters was calculated, and the cluster with the maximum sum was defined as the cluster-level statistic. Subsequently, we created 1000 random partitions of the real data (by shuffling the data of RAS and silent periods, and of targeted and untargeted hemispheres, respectively) and calculated the cluster-level test statistic in each random partition. This way, we obtained a histogram of the maximum sums of cluster *t*-values based on the random samples. We used this distribution as a reference to examine the statistics of the observed data. The proportion of random samples that yielded a larger cluster-level statistic than the observed one was defined as the significance probability. If this number was below 0.05, we considered the data of the two conditions as statistically significant [33].

In order to test whether coherence values between the acoustic pattern and the EEG signal were statistically significant, we created surrogate time series data for each trial, channel, and participant. We used the Amplitude Adjusted Fourier Transform algorithm that randomizes the phase of the signal but preserves the amplitude distribution of the original time series [34]. Coherence coefficients were computed similarly for the surrogate data and the acoustic signal. We used paired *t*-tests to compare coherence values of the observed and of the surrogate data, and addressed the issue of multiple comparisons by estimating the false discovery rate [35].

Results

Band-wise comparisons

First, we created a linear regression model with all variables that were relevant for the hypotheses (condition, band, side) using all main effects and interactions, and compared it to a linear mixed-effects model with random intercept for the participants and the number of trials. The comparison showed that the model applying a random intercept considerably increased the model fit. Next, we created a random intercept and slope model, in which we assumed a random slope by the factor condition. Adding a random slope did not improve the model. Therefore, we choose to use the random intercept as the final model (Table 1). We kept all fixed effects in the final model.

The main effect of condition was not significant ($b = –0.01$, $t = 0.05$, $p = 0.61$) indicating that RAS did not generally modify spectral power of all the examined frequency bands. Nevertheless, a significant interaction between condition and band emerged due to the selective enhancement of delta power during RAS compared to silent periods ($b = 0.073$, $t = 3.69$, $p < .001$). Post hoc comparisons of band-wise power spectra across RAS and silent conditions showed increased delta power during RAS compared to silent periods (Wilcoxon signed rank test = 582, CI [12.74;39.72], $p < 0.001$). Contrasts in other frequency bands were not significant (Figure 2). With regard to our second hypothesis, the three-way interaction between condition, band and side was not significant, and there was no sign of selective increase in delta power during RAS within the targeted hemisphere ($b = –0.005$, $t = 0.19$, $p = 0.850$). Accordingly, explorative post hoc comparisons contrasting the change in spectral power as a function of RAS (Figure 3) showed no significant differences in any frequency bands across the targeted and untargeted sides (all $p > 0.2$). Nonetheless, there was a significant side effect indicating a generally reduced spectral power within the targeted compared to the untargeted side, irrespective of condition and band, but this effect was not significant after correction for multiple comparisons. As expected, the main effect of band was significant during sleep: delta ($b = 2.661$, $t = 190.73$, $p < 0.001$) and theta ($b = 0.673$, $t = 48.208$, $p < 0.001$) power was larger, while beta ($b = –0.592$, $t = –42.40$, $p < 0.001$) and sigma ($–0.319$, $t = –22.83$, $p < 0.001$) power was lower (compared to alpha activity that was used as baseline) (Supplementary Figure S1; marginal $R^2 = .86$, conditional $R^2 = .91$). Standardized residuals for the linear mixed-effects model were investigated. The distribution of the residuals was unimodal and symmetrical; however, it was not normally distributed according to the Jarque-Bera normality (JB = 13230, $p < 0.001$) test. Nonetheless, this alteration is unlikely to affect the interpretation of results.

Bin-wise comparisons

Spectral power between 0.75 and 2.25 Hz was significantly higher during RAS compared to silent periods. As shown in Figure 4, the lowest frequencies exhibited a 10%–15% increase in spectral power during stimulation. Although frequencies in the

Table 1. Model comparison for different random structures

Models	df	AIC	BIC	logLik	Deviance	χ^2	Δdf	*p*
Linear regression with fixed terms only	21	243303	243478	–121631	243261.4			
Random intercept	23	27052	27243	–13503	27006.3	216255	2	<0.0001
Random intercept and slope	27	27057	27281	–13501	27002.6	3.709	4	0.4470

df = degrees of freedom; AIC = Akaike Information Criterion; BIC = Bayesian Information Criterion; logLik = likelihood ratio test; χ^2 = Chi-square. Model comparison showed that the random intercept model had the best fit, and that the random intercept and slope model did not considerably improve the model fit. *p* values correspond to the statistical comparisons of first and the second model, and of the second and the third model.

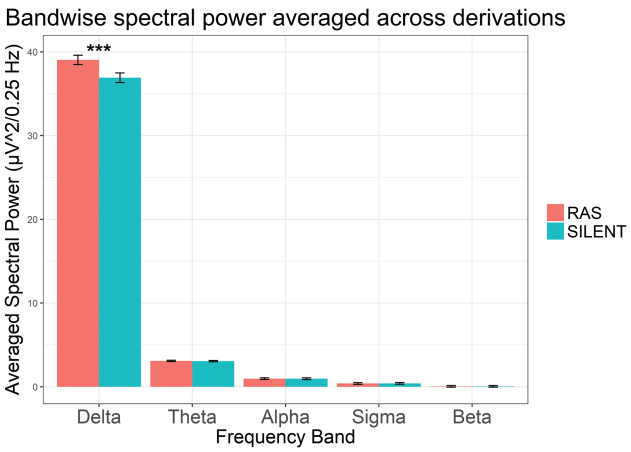

Figure 2. Absolute spectral power values during RAS and silent periods. The barplot shows mean values and standard errors of absolute spectral power in five frequency bands averaged across all electrodes. The two conditions were statistically different in case of delta band power (FDR-adjusted p value < 0.001).

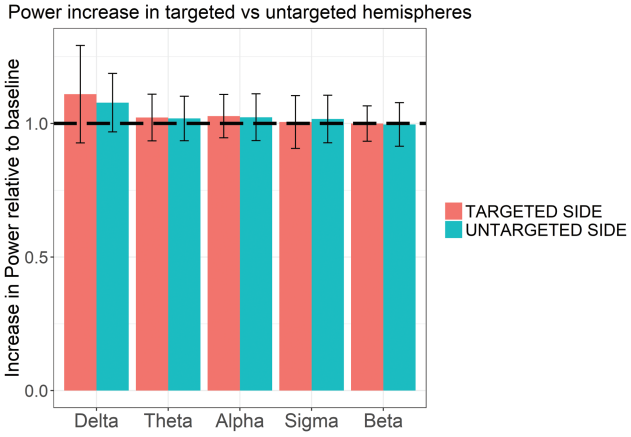

Figure 3. Change in average power spectra during RAS relative to silent periods. The barplot shows mean values and standard errors of the change in spectral power in five frequency bands averaged across electrodes lying within targeted and untargeted hemispheres. Values above the black, dashed line indicate an increase in spectral power relative to silent periods. No significant differences were found between the targeted and untargeted hemispheres.

alpha-sigma range (~12 Hz) were also higher during RAS, these differences were only trends and were only apparent in single frequency bins. In sum, bin-wise comparisons of spectral power between RAS and silent periods indicated that the increase in delta band power during stimulation was more prominent within the low-frequency components of delta activity.

In addition, we compared the relative increase in spectral power compared to the silent period within the targeted and untargeted hemispheres. No significant differences emerged between the targeted and untargeted sides after considering our criterion of at least three significant adjacent bins. Figure 5 shows the increase of spectral power relative to the silent periods within the targeted and untargeted sides, separately.

Temporal dynamics of slow frequency activity

The time-frequency analysis comparing RAS and silent periods showed significant increases in slow frequency oscillations

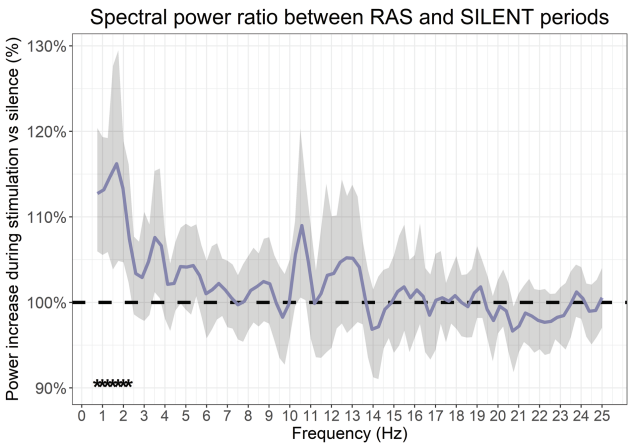

Figure 4. Spectral power ratio of RAS (Stimulation) and silent periods in each frequency bin. The line graph shows the averaged values across trials and electrode locations. The blue line (smoothed for visualization) depicts mean values, the shading indicates confidence intervals. Stars indicate significant bins, fulfilling the criteria for the correction of false positives (at least three significant adjacent bins).

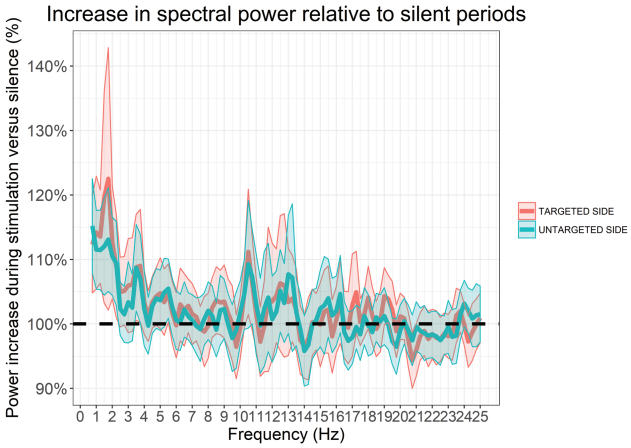

Figure 5. Relative increase in bin-wise spectral power values during RAS compared to silent periods within the targeted and untargeted hemispheres. The line plots depict mean values, the shading indicates confidence intervals.

during the first quarter (~3 seconds) of the stimulation reaching a 1.5-fold increase after the onset of RAS. Although slow frequency activity was relatively higher throughout the 12-second period of stimulation, significant clusters were restricted to the first 3 seconds from the onset of RAS. Furthermore, at the onset of RAS trials (corresponding to the first sound burst) a significant cluster was evidenced in the theta (5–8 Hz) and sigma (12–16 Hz) ranges that lasted 0.5 and 2 seconds, respectively (Figure 6).

In addition, we compared the time-frequency plots showing spectral power changes relative to silent periods within the targeted and untargeted hemispheres. Therefore, we first computed the change in power spectra in the corresponding electrode locations, and then contrasted these normalized values between the targeted and untargeted hemispheres by cluster-based permutation tests. No significant clusters emerged, indicating that the change in spectral power was not statistically different within the targeted and untargeted hemispheres.

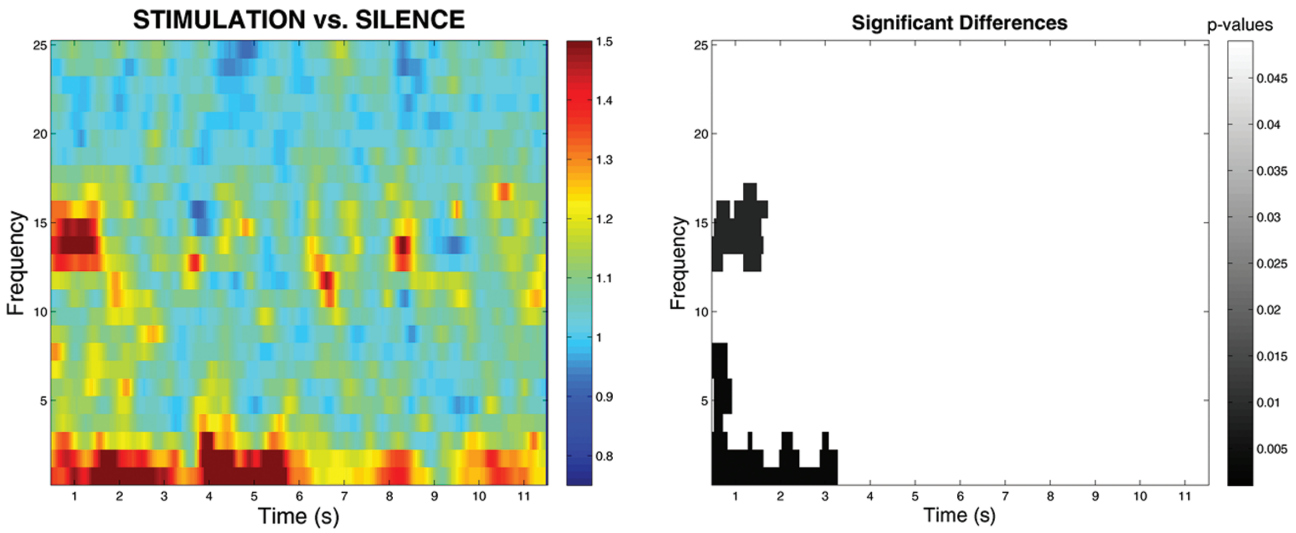

Figure 6. Temporal dynamics of relative increase in power spectra during RAS trials compared to silent periods. The time-frequency plot on the left contrasts spectral power values during RAS with that of silent periods. The heat map shows the mean values of the ratio of power spectra of Stimulated and silent conditions. Clusters of significant differences are illustrated on the right.

Phase coupling between the stimulation and the EEG signal

ITPC values were compared across RAS and silent periods for each EEG channel separately (Supplementary Figure S3/A). FDR adjusted, significant data points showed a sporadic distribution and no significant differences emerged after the more stringent cluster-based permutation test, suggesting that ITPC in different frequencies and time points were not different across RAS and silent periods (Supplementary Figure S3/B). Coherence coefficients between the acoustic stimulation and the EEG oscillations of 1 Hz frequency showed low values (spanning between 0.15 and 0.2), and were not statistically different from the coherence values between the acoustic signal and the surrogate data. These findings indicate that although slow oscillatory activity is enhanced during auditory stimulation, these oscillations are not phase coupled to the rhythm of the acoustic patterns.

Discussion

The aim of our study was to examine the effects of unilaterally presented rhythmic acoustic sound patterns on sleep EEG oscillations. Our data indicate that RAS of 1 Hz frequency, delivered in blocks of 12 seconds during daytime NREM sleep effectively enhances delta power in comparisons to baseline, non-stimulated periods. RAS with 1 Hz frequency during NREM sleep specifically increased slow oscillatory activity between 0.75 and 2.25 Hz, that is, the slower components of the traditionally defined delta band. This increase in slow oscillatory activity was apparent in both hemispheres, regardless of the side of the stimulation. The stimulation did not significantly increase the average spectral power of other frequency bands within the analyzed frequency range (0.75–25 Hz); however, the temporal dynamics of power fluctuations showed short-lasting, but significant increases of frequencies beyond the delta range. More specifically, there was an increase in theta (up to 8 Hz) and sigma (12–16 Hz) power immediately after the first pulse of stimulation that ceased after the second pulse, and was no longer evident during the RAS period.

Our findings add to the growing number of evidence showing the effectiveness of acoustic stimulation in enhancing slow wave activity [9, 10, 12, 13, 15]. Although the occurrence of large amplitude slow waves (K-complexes) in response to sensory stimulation was first described 80 years ago [36], the potential of acoustic stimulation to increase slow oscillatory activity without eliciting arousals or micro-awakenings is still a matter of future research [8]. One line of research aims to optimize the timing of delivered sound pulses by presenting the stimuli during the up states of SOs [9, 10, 13]. The advantage of this procedure is that auditory stimulation usually consisting of short (~50 ms) acoustic events always arrive at the depolarizing phase of thalamo-cortical oscillations when the neuronal populations are responsive to auditory stimulation, and hence, stimulation is ceased at the phases of hyperpolarized down states that are characterized by a certain degree of nonresponsiveness. Accordingly, tones delivered during the (depolarizing) up states enhanced SOs between 0.5 and 1 Hz by approximately 9%, but disrupted SOs when they were presented after the negative half-wave (hyperpolarized, down state) of SOs [9].

In this study, we did not focus on the timing of acoustic stimulation, but aimed to exploit the brain's tendency to entrain to repetitive stimulation [8]. Neural entrainment by repetitive stimulation was previously evidenced during sleep [8, 11], and was not restricted to the auditory domain [37]. Here, instead of short-lasting tones, we modulated the amplitude of pink noise by 1 Hz frequency that resulted in a stream of stimulation consisting of repetitive sound bursts of rising and falling intensity. We achieved to increase average delta power (0.75–4 Hz) by approximately 8% during the stimulated periods in comparison with the non-stimulated ones. Moreover, bin-wise analyses of the effect of stimulation indicate that the highest increases in power (up to 15%) were apparent within the slower frequency range (0.75–2.25 Hz). This pattern of findings is in contrast with the results of Ngo and colleagues [9] showing stimulation-dependent enhancement particularly in (0.5–1 Hz) SOs, and a significant decrease in neighboring (1–4 Hz) frequency bands. We may speculate that protocols focusing on the timing of auditory stimulation, that is, on the presentation of acoustic stimuli at the up-states of SOs might

principally evoke additional SOs (such as K-complexes), whereas procedures of rhythmic entrainment presenting longer sequences of stimulation might additionally boost oscillations of neighboring frequencies due to the natural jittering (dynamic changes) of oscillatory activity. This assumption is in line with the findings of other studies that aimed to take advantage of both the timing and the resonant properties of RAS, and similarly to our results showed increased power in neighboring frequencies [13, 15].

Although slow oscillatory activity was enhanced during RAS, oscillatory activity was not phase synchronized to the 1 Hz rhythm of the auditory stimuli. ITPC was different between RAS and silent periods, suggesting that the acoustic stimulation did not influence the phases of oscillatory activity in a consistent manner. This uncoupling between the auditory stimulation and the EEG oscillations was also corroborated by coherence analyses showing no significant synchronization between the acoustic stimuli and the EEG oscillations of 1 Hz. In light of these findings it is worth considering whether the term "entrainment" is appropriate. Indeed, despite boosting slow waves, RAS does not appear to entrain the phase of such oscillations. However, a study by Ong and colleagues [13] suggests that closed-loop acoustic stimulation might be more effective in producing slow oscillatory activity that is phase-locked across trials.

It is important to note here, that the lack of entrainment suggests that delta band power can be increased by different kinds of stimulations including sounds without rhythmic properties [38], or RAS of other (higher) frequencies [39]. For instance, in a recent study Lustenberger and colleagues showed an increase in 1–7 Hz slow frequency oscillations by RAS of faster (14 Hz and 40 Hz) frequencies. More importantly, they showed that ITPC varies as a function of sleep pressure and ongoing SOs [39]. As slow waves and delta power can be enhanced by different procedures during NREM sleep, our 1-Hz RAS is certainly not an unequivocally specific stimulation to elicit slow frequency oscillations. The resonant properties of the sleeping brain, as well as the specificity of elicited and enhanced oscillations, should be explored by future studies that examine the effects of RASs of different frequencies and contrast these procedures with non-rhythmic auditory stimulations.

The analysis of the temporal dynamics of RAS revealed that the most robust increases in slow oscillatory activity appeared during the first 3 seconds of the stimulation period. Although spectral power in low-frequency activity seemed to be higher throughout the 12-second long stimulation period, these differences were not significant after correction for multiple comparisons. The relative increase in delta power limited to the first quarter of RAS is in line with a study showing a certain degree of refractoriness after sustained stimulation [40]. The refractoriness of evoked potentials during sleep was described in the first studies focusing on K-complexes [41], and was more systematically examined by Bastien and Campbell [42] who presented tones at different rates during NREM sleep and showed that the N350 and N550 components of the evoked K-complexes are clearly affected by refractory periods [42]. In addition, the temporal pattern of enhanced delta power coheres with other reports showing an increase in slow oscillatory activity during the first 3–4 seconds of sustained stimulation [13, 14]. In addition, a short-lasting increase in theta (5–8 Hz) and sigma (12–16 Hz) power occurred during the first pulse of RAS. The increase in theta power was also evidenced in a recent study that applied phase-locked RAS of five consecutive pulses during a daytime nap [13]. These findings indicate that low-frequency acoustic stimulation might have an effect on oscillatory activity beyond the targeted frequency. Theta oscillations during NREM sleep does not seem to be independent from delta wave activity as theta band power is also increased after prolonged wakefulness during recovery NREM sleep, suggesting that the homeostatic mechanism of sleep is not restricted to delta wave activity [43]. The short-lasting increase in sigma power immediately after the first pulse of stimulation might reflect sleep spindles that are often superimposed on evoked K-complexes [44].

Our hypothesis assuming that lateralized RAS would have a stronger effect on the electrode locations contralateral to the stimulated side was not supported by the present results. Earlier studies indicated that unilaterally presented auditory evoked potentials exhibited larger amplitudes in the contralateral hemisphere, arguing for the phenomenon of contralateral dominance of auditory neural pathways [45]. Furthermore, slow oscillatory activity can be expressed in a region-specific manner as a function of prior activity during wakefulness [16, 17]. These findings indicate that the neural state of sleep has local properties beyond the more global and behaviorally evident aspects of sleep [6]. Finally, studies reporting cerebral asymmetries in arousals, in evoked auditory responses, and in slow oscillatory activity suggest that the two hemispheres might exhibit different auditory connection with the external environment [18, 19, 46]. In contrast to these intriguing data, our procedure of lateralized RAS did not produce a differential effect on the targeted hemisphere compared to the nontargeted one. We propose that the laterality effect is more subtle and localized, and thus might require more electrode contacts or intracranial electrodes in order to be detectable. Furthermore, cerebral dominance is characterized by spontaneous ultradian fluctuations that might have masked the lateral effects of stimulation, therefore, future studies should take into account the ultradian effects of cerebral dominance [47]. Another, alternative explanation for the lack of local effects is that the increase in SOs is triggered by the diffuse activity of some of the critical portions of the reticular ascending arousal system, and is not directly related to the activity of the specific thalamo-cortical auditory pathways [8, 48]. In fact, such mechanism might explain a lack of phase coupling between the auditory stimulation and the enhanced oscillations.

The most evident limitation of our study is the low number of electrodes. Future studies applying high-density EEG might be more effective in revealing contralateral dominance in unilaterally enhanced slow oscillatory activity. Furthermore, as the principal aim of our study was to examine the difference between stimulated and unstimulated periods of NREM sleep, we did not apply control measurements with sham stimulation, and hence, we are unable to link the efficacy of RAS to changes in subjective sleep quality. In spite of these limitations, our findings indicate that lateralized RAS has a strong potential to enhance slow waves during daytime naps, particularly during the first 3–4 seconds of stimulation.

Supplementary material

Supplementary material is available at *SLEEP* online.

Funding

The project was partially supported by the Belgian Fonds National de la Recherche Scientifique with FRS-FNRS grant T.109.13 and,

by the Eötvös Hungarian State Scholarship (2015/2016) of the Tempus Public Foundation. P.S. and P.P.U. were supported by the ÚNKP-17-4 New National Excellence Program of the Ministry of Human Capacities. At the time the study was conducted R.S. was a F.R.S.-FNRS Postdoctoral Researcher and M.G. and J.F. were F.R.S.-FNRS Doctoral Researchers (Research Fellows).
Conflict of interest statement. None declared.

References

1. Achermann P, *et al*. A model of human sleep homeostasis based on EEG slow-wave activity: quantitative comparison of data and simulations. *Brain Res Bull*. 1993;**31**(1–2):97–113.
2. Bazhenov M, *et al*. Model of thalamocortical slow-wave sleep oscillations and transitions to activated states. *J Neurosci*. 2002;**22**(19):8691–8704.
3. Steriade M, *et al*. Thalamocortical oscillations in the sleeping and aroused brain. *Science*. 1993;**262**(5134):679–685.
4. Borbély AA, *et al*. The two-process model of sleep regulation: a reappraisal. *J Sleep Res*. 2016;**25**(2):131–143.
5. Rasch B, *et al*. About sleep's role in memory. *Physiol Rev*. 2013;**93**(2):681–766.
6. Tononi G, *et al*. Sleep function and synaptic homeostasis. *Sleep Med Rev*. 2006;**10**(1):49–62.
7. Holz J, *et al*. EEG sigma and slow-wave activity during NREM sleep correlate with overnight declarative and procedural memory consolidation. *J Sleep Res*. 2012;**21**(6):612–619.
8. Bellesi M, *et al*. Enhancement of sleep slow waves: underlying mechanisms and practical consequences. *Front Syst Neurosci*. 2014;**8**:208.
9. Ngo HV, *et al*. Auditory closed-loop stimulation of the sleep slow oscillation enhances memory. *Neuron*. 2013;**78**(3):545–553.
10. Santostasi G, *et al*. Phase-locked loop for precisely timed acoustic stimulation during sleep. *J Neurosci Methods*. 2016;**259**:101–114.
11. Antony JW, *et al*. Using oscillating sounds to manipulate sleep spindles. *Sleep*. 2017;**40**(3). doi:10.1093/sleep/zsw068
12. Ngo HV, *et al*. Induction of slow oscillations by rhythmic acoustic stimulation. *J Sleep Res*. 2013;**22**(1):22–31.
13. Ong JL, *et al*. Effects of phase-locked acoustic stimulation during a nap on EEG spectra and declarative memory consolidation. *Sleep Med*. 2016;**20**:88–97.
14. Papalambros NA, *et al*. Enhancing slow-wave activity in mild cognitive impairment using acoustic stimulation during sleep. *Sleep Med*. 2017;**40** (Suppl. 1):e251–e252.
15. Papalambros NA, *et al*. Acoustic enhancement of sleep slow oscillations and concomitant memory improvement in older adults. *Front Hum Neurosci*. 2017;**11**:109.
16. Hung CS, *et al*. Local experience-dependent changes in the wake EEG after prolonged wakefulness. *Sleep*. 2013;**36**(1):59–72.
17. Krueger JM, *et al*. A neuronal group theory of sleep function. *J Sleep Res*. 1993;**2**(2):63–69.
18. Rattenborg NC, *et al*. Behavioral, neurophysiological and evolutionary perspectives on unihemispheric sleep. *Neurosci Biobehav Rev*. 2000;**24**(8):817–842.
19. Tamaki M, *et al*. Night watch in one brain hemisphere during sleep associated with the first-night effect in humans. *Curr Biol*. 2016;**26**(9):1190–1194.
20. Nicholls ME, *et al*. The Flinders Handedness survey (FLANDERS): a brief measure of skilled hand preference. *Cortex*. 2013;**49**(10):2914–2926.
21. Beck AT, *et al*. Psychometric properties of the beck depression inventory: twenty-five years of evaluation. *Clin Psychol Rev*. 1988;**8**(1):77–100.
22. Buysse DJ, *et al*. The Pittsburgh sleep quality index: a new instrument for psychiatric practice and research. *Psychiatry Res*. 1989;**28**(2):193–213.
23. Jasper H. Report of the committee on methods of clinical examination in electroencephalography. *Electroencephalogr Clin Neurophysiol*. 1958;**10**:370–375.
24. Berry RB, *et al*.; American Academy of Sleep Medicine. Rules for scoring respiratory events in sleep: update of the 2007 AASM manual for the scoring of sleep and associated events. Deliberations of the sleep apnea definitions task force of the American Academy of Sleep Medicine. *J Clin Sleep Med*. 2012;**8**(5):597–619.
25. Oostenveld R, *et al*. FieldTrip: open source software for advanced analysis of MEG, EEG, and invasive electrophysiological data. *Comput Intell Neurosci*. 2011;**2011**:156869.
26. van Diepen RM, *et al*. The Caveats of observing inter-trial phase-coherence in cognitive neuroscience. *Sci Rep*. 2018;**8**(1):2990.
27. Papenberg G, *et al*. Lower theta inter-trial phase coherence during performance monitoring is related to higher reaction time variability: a lifespan study. *Neuroimage*. 2013;**83**:912–920.
28. Delorme A, *et al*. EEGLAB: an open source toolbox for analysis of single-trial EEG dynamics including independent component analysis. *J Neurosci Methods*. 2004;**134**(1):9–21.
29. Bastos AM, *et al*. A tutorial review of functional connectivity analysis methods and their interpretational pitfalls. *Front Syst Neurosci*. 2015;**9**:175.
30. R Core Team. *R: A Language and Environment for Statistical Computing*. Vienna, Austria: R Foundation for Statistical Computing; 2014.
31. Zuur AF, *et al*. Zero-truncated and zero-inflated models for count data. In: *Mixed Effects Models and Extensions in Ecology with R*. New York: Springer-Verlag; 2009: 261–293.
32. Tarokh L, *et al*. Developmental changes in brain connectivity assessed using the sleep EEG. *Neuroscience*. 2010;**171**(2):622–634.
33. Maris E, *et al*. Nonparametric statistical testing of EEG- and MEG-data. *J Neurosci Methods*. 2007;**164**(1):177–190.
34. Theiler J, *et al*. Testing for nonlinearity in time series: the method of surrogate data. *Phys Nonlinear Phenom*. 1992;**58**(1):77–94.
35. Benjamini Y, *et al*. Controlling the false discovery rate: a practical and powerful approach to multiple testing. *J R Stat Soc Ser B Methodol*. 1995;**57**(1):289–300.
36. Loomis AL, *et al*. Distribution of disturbance-patterns in the human electroencephalogram, with special reference to sleep. *J Neurophysiol*. 1938;**1**(5):413–430.
37. Bayer L, *et al*. Rocking synchronizes brain waves during a short nap. *Curr Biol*. 2011;**21**(12):R461–R462.
38. Halász P, *et al*. Two features of sleep slow waves: homeostatic and reactive aspects–from long term to instant sleep homeostasis. *Sleep Med*. 2014;**15**(10):1184–1195.
39. Lustenberger C, *et al*. High-density EEG characterization of brain responses to auditory rhythmic stimuli during wakefulness and NREM sleep. *Neuroimage*. 2018;**169**:57–68.
40. Ngo HV, *et al*. Driving sleep slow oscillations by auditory closed-loop stimulation-a self-limiting process. *J Neurosci*. 2015;**35**(17):6630–6638.
41. Colrain IM. The K-complex: a 7-decade history. *Sleep*. 2005;**28**(2):255–273.

42. Bastien C, *et al*. Effects of rate of tone-pip stimulation on the evoked K-Complex. *J Sleep Res*. 1994;**3**(2):65–72.
43. Marzano C, *et al*. The effects of sleep deprivation in humans: topographical electroencephalogram changes in non-rapid eye movement (NREM) sleep versus REM sleep. *J Sleep Res*. 2010;**19**(2):260–268.
44. Halász P. The K-complex as a special reactive sleep slow wave - a theoretical update. *Sleep Med Rev*. 2016;**29**:34–40.
45. Connolly JF. Stability of pathway-hemisphere differences in the auditory event-related potential (ERP) to monaural stimulation. *Psychophysiology*. 1985;**22**(1):87–95.
46. Armitage R, *et al*. Asymmetrical auditory probe evoked potentials during REM and NREM sleep. *Sleep*. 1990;**13**(1):69–78.
47. Shannahoff-Khalsa DS, *et al*. Ultradian rhythms of alternating cerebral hemispheric EEG dominance are coupled to rapid eye movement and non-rapid eye movement stage 4 sleep in humans. *Sleep Med*. 2001;**2**(4):333–346.
48. Berlucchi G. One or many arousal systems? Reflections on some of Giuseppe Moruzzi's foresights and insights about the intrinsic regulation of brain activity. *Arch Ital Biol*. 1997;**135**(1):5–14.